

**ALTERATIONS IN THE MICROSTRUCTURE OF THE ANTERIOR MITRAL VALVE LEAFLET UNDER PHYSIOLOGICAL STRESS**

**Christopher A. Carruthers (1), Bryan Good (1), Antonio D'Amore (1-3), Jun Liao (4), Rouzbeh Amini (1), Simon C. Watkins (5), Michael S. Sacks (6)**

Department of Bioengineering  
University of Pittsburgh  
Pittsburgh, PA 15219

(2) Fondazione RiMED  
Palermo, Italy 90134

(3) Dipartimento di Ingegneria Industriale  
University of Palermo  
Palermo, Italy 90128

(4) Department of Biomedical Engineering  
Mississippi State University  
Mississippi State, MS

(5) Department of Cell Biology and Physiology  
University of Pittsburgh  
Pittsburgh, PA

(6) Department of Biomedical Engineering  
University of Texas  
Austin, Texas

**INTRODUCTION**

An improved understanding of mitral valve (MV) function remains an important goal for determining mechanisms underlying valve disease and for developing novel therapies. Critical to heart valve tissue homeostasis is the valvular interstitial cells (VICs), which reside in the interstitium and maintain the extracellular matrix (ECM) through both protein synthesis and enzymatic degradation [1]. There is scant quantitative experimental data on the alterations of the MV fiber network reorganization as a function of load, which is critical for implementation of computational strategies that attempt to link this meso-micro scale phenomenon. The observed large scale deformations experienced by VICs could be implicated in mechanotransduction [2], i.e., translation of mechanical stimuli into biochemical signals. Consequently, our goal was to quantitatively characterize the MV microstructure as a function of physiological loads, including localized 3D VIC deformations and relate it to the fiber network.

**MATERIALS & METHODS**

To establish a quantitative basis for this hypothesis, we applied physiologic biaxial loads to the anterior mitral valve (MV) leaflet. We then acquired and analyzed cellular deformations and related them to changes in local fiber microstructure utilizing a multiphoton microscope (MPM). Ovine anterior MV leaflets, approximately 35 kgs in size, were acquired and a 1 cm x 1 cm sample was mounted into a miniature biaxial testing system. An equibiaxial tension path was chosen wherein the ratio of axial tension was maintained. The maximum tension level was set to 150 N/m, with a total of seven tension points chosen for the loading path, with one specimen used per tension level. Samples were both imaged in real time en-face, and fixed at the desired tension level in 2% PFA for 2 hours, sectioned, and imaged along the transverse-circumferential axis.

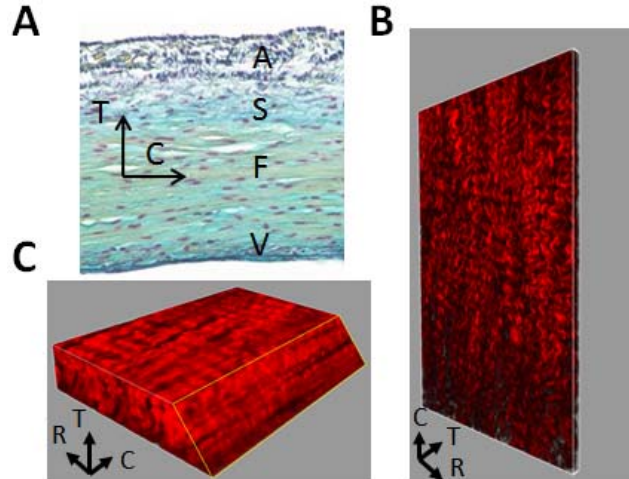


**Figure 1: (A) Movats section indicating tri-layered structure, (B) 3D reconstruction of collagen fibers of atrialis, (C) and fibrosa. C, R, T represent circumferential, radial and transverse direction, respectively. A, S, F, V represent the atrialis, spongiosa, fibrosa, and ventricularis layer, respectively.**

Fixed samples were split into two pieces with long-axis oriented along the circumferential direction. The first piece was embedded into OCT for transverse sectioning. A 30  $\mu$ m cryosection was also taken for MPM to identify collagen fibers from second harmonic generation (SHG), and cell nuclei from a cytox green stain. Samples were imaged en-face to 100  $\mu$ m deep from both the atrialis and ventricularis surface to encompass all layers. The second intact piece was cleared using

glycerol and then scanned using small angle light scattering technique (SALS) to acquire collagen fiber orientation for the entire volume [3].

From the 30  $\mu\text{m}$  transverse cryosection image stack nuclei were reconstructed to determine cellular deformation, and orientation. Collagen and elastin fiber direction, and orientation index was automatically detected from layer specific z-projections using a previously developed algorithm by our lab [4]. The observable collagen fiber straightening was also measured from z-projections. The amplitude of the collagen fibers for both the atrialis and fibrosa was measured from 3D stacks in the free float configuration.

## RESULTS

Upon investigation of the layer dependent collagen fiber architecture in the free float configuration (Fig 1A-C) we observed that the fibers of the atrialis layer were less dense, individually identifiable, and oriented in the circumferential-radial plane, while those of the fibrosa layer were bundles of sheets oriented in the transverse-radial plane. The atrialis fibers also had two times higher amplitude than the fibrosa fibers, although both fiber populations had similar periods.

The collagen and elastin network (Fig 2A-B) was also quantified as a function of increasing tension for all layers. The collagen fiber straightening was found to be nonlinear with a sharp increase from 0 to 20 N/m (Fig 2C). Fiber direction did not change with tension, but was found to be different as a function of layer with the spongiosa being least organized (Fig. 2D). The preferred fiber direction for the atrialis layer was along the radial direction, while for the fibrosa and ventricularis layer it was along the circumferential direction (Fig. 2A-B, E). This observation was confirmed with SALS as seen by the two distinct fiber populations (Fig. 2F). This finding of two directionally opposing elastin networks on opposite valve surfaces motivates further examination into the closure mechanics of the MV as a function of its complex hierarchical structures that may potentially be answered through computational simulations.

Results indicated that the MV anterior leaflet had a nonlinear-layer dependent cellular deformation response. The VICs in the collagen rich fibrosa layer reaching the highest deformation level, and were found to orient along the circumferential direction (Fig. 3A-B). The observed VIC fibrosa deformation and alignment response correlated closely with local fiber straightening suggesting that the mechanism of cellular deformation was due to a localized collagen fiber compaction of the cell.

## DISCUSSION

For the first time MV collagen and elastin fiber kinematics and cell deformation was quantified under controlled biaxial loading to physiological levels. We found deformation level and layer dependence, with the cellular deformation highest in the fibrosa layer that is mainly composed of collagen type I. The cellular deformation correlated closely with collagen fiber reorientation and straightening with load. A novel finding was the two opposing fiber networks on opposite sides of the leaflet, which may functionally allow for greater controllability over two axes of flexure and may be related to the saddle shape of the leaflet. These subtle layer differences in ECM planar organization, and the intricate interrelationship between ECM planar organization and VIC deformation indicate the necessity to account for micro-meso scale phenomena when developing MV finite element models. The long-term goal is for these findings to provide insight into VIC mechanobiology as a function of ECM architecture under organ level loads. ECM architecture has been shown to change with age, disease, and repair with procedures such as annuloplasty and resection. Hence, these experimental findings will motivate a structurally accurate MV model to investigate VIC deformation as a

function of layer specific ECM planar organization under organ level loads.

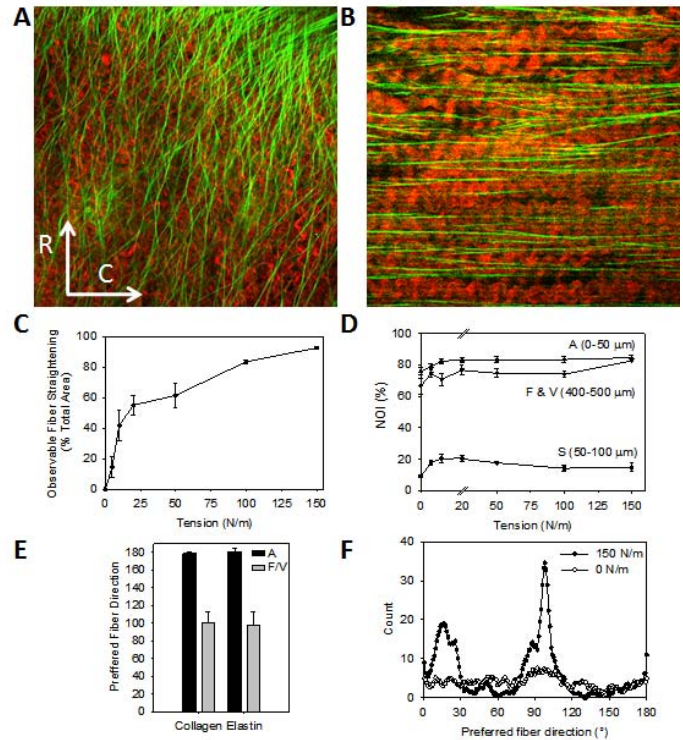


**Figure 2: En-face image of collagen (red) and elastin (green) oriented orthogonally to each other for the (A) atrialis and the (B) ventricularis, (C) Collagen fiber straightening in the transverse-circumferential plane, (D) normalized orientation index (NOI) for the atrialis, spongiosa, fibrosa, and ventricularis, (E) preferred fiber direction from both MPM and (F) SALS indicating two distinct fiber populations.**

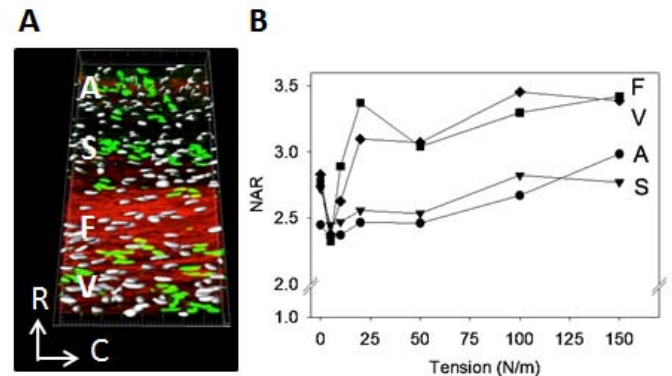


**Figure 3: (A) MPM stack reconstruction with collagen (red) and cell nuclei (green) for the loaded configuration. T and C represent transverse and circumferential direction, respectively. (B) Nuclear aspect ratio as a function of layer and tension. A, S, F, V represent the atrialis, spongiosa, fibrosa, and ventricularis layer, respectively.**

## ACKNOWLEDGMENTS

Greg Gibson for help with MPM, and R01 HL-688116, NIBIB T32 EB003392-03, NSF-GRFP 2009068895

## REFERENCES

1. Taylor, P.M., et al., *IJBCB*, 35: p. 113-8, 2003.
2. Xing, Y., et al., *ABME*, 32: p. 1461-70, 2004.
3. Sacks, M.S., et al., *ABME*, 25: p. 678-89, 1997.
4. D'Amore, A., et al., *Biomaterials*, 31: p. 5345-54, 2010.